Experimental and Numerical Study of Surface Nitridation of Thermal Protection Material

Toshiyuki Suzuki* and Kazuhisa Fujita†
Japan Aerospace Exploration Agency, Tokyo, 182-0012, Japan

and

Takeharu Sakai‡
Nagoya University, Aichi, 464-8603, Japan

Nitridation of graphite is observed in the inductively coupled plasma heated wind tunnel. Probability values of nitridation reaction are determined from the amount of mass loss of graphite test piece and atomic nitrogen density in the test section. The amount of atomic nitrogen is determined by calculating the flowfield around the graphite test piece under wind tunnel freestream condition. The freestream condition at the entrance of test chamber is evaluated by calculating the flows in the plasma toarch fully theoretically. It is found from experimental and numerical results that the reaction probability is about 0.003 for the surface temperature of about 1900K. The uncertainties in the results are also described, and improvements are proposed.

Nomenclature

A	=	surface area of graphite test piece, 2.43×10^{-4} m^2
k	=	surface reaction velocity, m/s
M_s	=	molecular weight of species s, kg/mol
R	=	universal gas constant, 8.314 J/(mol-K)
r	=	mass loss rate, kg/s
T	=	temperature, K
α	=	reaction probability
ρ_s	=	density of species s, kg/m^3

I. Introduction

In Japan, there has been an increasing interest for planetary entry missions. Well known examples are sample return mission named HAYABUSA (MUSES-C)[1] and Unmanned Space Experiment Recovery System (USERS)[2]. When the entry capsule enters into Earth's atmosphere along the hyperbolic trajectory, the absolute velocity of the capsule exceeds about 12km/s. At such flight velocity, the flow temperature behind a detached shock wave becomes so high that air molecules can be vibrationally excited, dissociated, or ionized. In these missions, therefore, a carbon fiber reinforced plastic (CFRP) ablator that consists of a base carbon fiber matrix and a resin is employed as the material of a thermal protrection system (TPS). When the virgin material of the ablator is heated, the resin decomposes and a pyrolysis gas is formed within the ablator. The pyrolysis gas then flows toward a wall surface and is released into the boundary layer. In the boundary layer, atomic oxygen and nitrogen so dissociated will reach the ablating surface. Because the ablating surface becomes nearly pure carbon due to the pyrolysis process, the solid carbon on the surface is oxidized or is nitrided by the atomic species in the boundary layer resulting in surface recession of the TPS material. Therefore, an estimation of the amount of surface recession is one of main subjects to designing the TPS of entry capsules.

*Researcher, Institute of Aerospace Technology, 7-44-1 Jindaiji Higashi-machi, Chofu-shi, Tokyo 182-8522, E-Mail: suzuki.toshiyuki@jaxa.jp
† Senior Researcher, Institute of Aerospace Technology, 7-44-1 Jindaiji Higashi-machi, Chofu-shi, Tokyo 182-8522
‡ Assistant Professor, Department of Aerospace Engineering, Furo-cho, Chikusa-ku, Nagoya, Aichi 464-8603

A considerable amount of effort has been expended to determine how fast the material surface recedes at high temperature.[3-6] It is well known that the atomic oxygen reacts with solid carbon to form gaseous CO through the oxidation process,

$$O + C(s) \rightarrow CO + 3.74ev\,. \tag{1}$$

The speed of the oxidation is expressed by a reaction probability, which is defined as the ratio of the mass flux of oxygen contained in the reaction product to the mass flux of oxygen reaching the wall surface. In Refs. 3-5, the reaction probability of oxidation reaction has been measured in atomic beam experiments. In such experiments, a beam of atomic oxygen was made to hit a solid carbon surface, and the flux of the product of the surface reaction was measured. From these experiments, the reaction probability of oxidation was found to vary from 0.01 to 0.3 depending on the material temperature. The obtained data were approximated in Ref. 7 as following,

$$\alpha = 0.63\exp\left(-\frac{1160}{T}\right). \tag{2}$$

The expression of Eq. (2) has been widely used to estimate the mass loss and the amount of recession due to oxidation reaction.[8, 9]

Recently, the probability of reaction of nitrogen atoms with solid carbon to form gasceous CN,

$$N + C(s) \rightarrow CN + 0.35ev\,, \tag{3}$$

was experimentally determined by Park and Bogdanoff.[6] This process was so-called nitridation reaction. In the experiment, a stream of highly dissociated nitrogen was produced in a shock tube and passed over a grid of metal wire coated with carbon. The reaction probability of nitridation reaction was determined by comparing the number density of CN molecules, determined from the measured intensity of CN radiation, with the calculated number density of atomic nitrogen in the wake of a grid of metal. From the measurement, the reaction probability is deduced to be about 0.3. However, questions remain as to how well the reaction probability reproduce the amount of mass loss of the material in an actual heating environment of interest.

The aim of the present study is to observe the nitridation phenomenon in a high enthalpy wind tunnel facility. For this purpose, heating tests using a graphite test piece are conducted in a 110kW inductively coupled plasma (ICP) heated wind tunnel installed in the Institute of Aerospace Technology (IAT) of Japan Aerospace Exploration Agency (JAXA). In the heating tests, pure nitrogen is used as a working gas. The amount of mass loss of graphite test piecies due to the nitridation reaction is examined by comparing weights of test piece between before and after heating tests. In order to discuss the nitridation reaction occurred at the test piece surface in this study, and to determine the nitridation reaction probability from the obtained data, we need to know the properties of flowfield around the test piece in detail. For this purpose, the flowfield around the test piece is calculated using the thermo-chemical nonequilibrium CFD code under an wind tunnel freestream condition. The freestream condition is evaluated by calculating the flows in the ICP heater fully theoretically. Finally, we attempt to estimate the reaction probability of the nitridation. The obtained values are then compared with those obtaied by Park and Bogdanoff.

II. Experimental Configurations

The schematic diagram of the 110kW ICP heated wind tunnel facility in IAT of JAXA is given in Fig. 1. The facility consists mainly of a plasma torach and a test chamber. The plasma toarch consists of a cylindrical discharge chamber made of a quartz tube and an induction coil of three-turn. A working gas is introduced from upstream wall, and is then discharged by supplying a radio-frequency current to the induction coil. The hot gas then flows into a test chamber. The quarts tube has a diameter of 75 mm and a length of 250 mm. The radio-frequency generator can work at power between 70 and 110kW at a frequency of 1.78MIIz.

A pure nitrogen is used as a wotking gas in this study to observe the nitridation reaction occurred at graphite surface. As pointed out by Ref. 10, however, impurities such as oxygen and hydrogen may remain in the test section to some extent because the test chamber can not be completely evacuated. In that case, we can not tell the nitridation reaction occurred at test piece surface from another reactions. In order to avoid such situation, impurities in the test chamber was substituted by nitogen gas three times (pressure ratio=30) before ignition of the plasma toarch. By conducting this substitution, the amount of impurities in the test chamber becomes lower by about $(1/30)^3$=1/27000 than those without conducting the substitution.

A photograph of test piece used in this study is shown in Fig. 2. A flat-faced rodded graphite test piece has a diameter of 3 mm and has a length of 50 mm, and is mounted on a firebrick attachment. A length and area of the graphite test piece that exposed to hot nitrogen gas is 25 mm and 2.43×10^{-4} m^2, respectively. In the present study,

surface temperature of the graphite test piece is measured by a one-color optical pyrometer. Test conditions and the wind tunnel operational parameters are summarized in Table 1. The measurements were made at 566 mm from the quartz tube exit. The working power used in this study is 70 kW and the mass flow rate of working gas is 1.8 g/s, realizing a mass-averaged enthalpy of about 15 MJ/kg. The mass-averaged enthalpy values were determined by using an energy balance method. The heat flux measurements were made using a Gardon gauge.

In this study, the reaction probability of nitridation is estimated by using the amount of mass loss of graphite test piece after the heating test. The methodology used in this study is as follows. The surface reaction velocity is given by kinetic theory as

$$k = \frac{\alpha}{4}\sqrt{\frac{8RT}{\pi M_N}} \ . \tag{4}$$

Thus, the mass loss rate of graphite test piece due to nitridation reaction is given by

$$r = \frac{M_C}{M_N} A \rho_N \frac{\alpha}{4}\sqrt{\frac{8RT}{\pi M_N}} \ . \tag{5}$$

Because there is no other experimental information for the atomic nitrogen density ρ_N at this time, the solution obtained by numerical analysis is used in this study. It should be noted in Eq. (5) that constant surface temperature and surface area of test piece are assumed during the heating tests. This point will be discussed later.

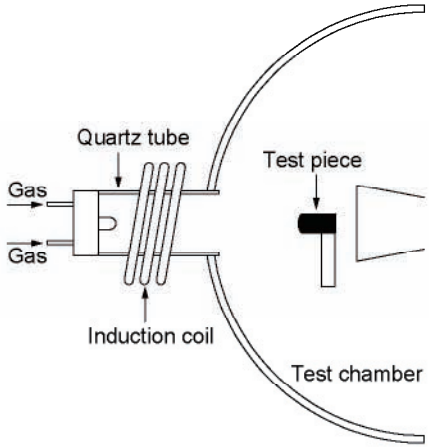

Fig. 1 Schematic of 110kW ICP heated wind tunnel facility installed in ISAS of JAXA.

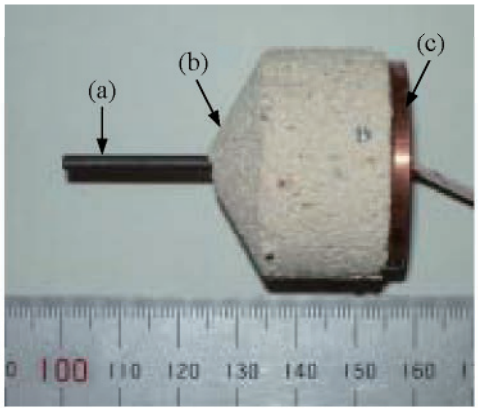

Fig. 2 Photograph of test piece used in this study; (a) graphite, (b) firebrick attachment, and (c) interface plate made of copper.

Table 1 Wind tunnel test conditions

Test piece No.	1	2	3	4
Working gas	N_2	N_2	N_2	N_2
Input power, [kW]	70	70	70	70
Mass flow rate, [g/s]	1.8	1.8	1.8	1.8
Ambient pressure, [kPa]	10	10	10	10
Heat flux, [MW/m^2]	0.7	0.7	0.7	0.7
Mass-averaged enthalpy, [MJ/kg]	15	15	15	15
Exposure time, [s]	600	900	900	1200

III. Numerical Methods

Two computational blocks are built to calculate the flowfield in the ICP heated wind tunnel: (1) simulation of the entire flowfield in the plasma toarch; and (2) simulation of flowfield over a graphite test piece in the test chamber.

A. Plasma Toarch Analysis Code

The inductively coupled plasma wind tunnel flowfield is calculated using a computational fluid dynamic(CFD) technique. An axisymmetric viscous flow is assumed to be thermochemical equilibrium, because pressure is 10kPa for typical operating conditions. Nitrogen is used as a test gas in the present study, and 5 chemical species model (N, N^+, N_2, N_2^+ and e-) is employed to account for high temperature phenomena. Mass, Momentum, and total energy conservation equations are solved using a finite volume method. Solutions are obtained by numerically integrating the equations in time to steady state by using mass flow rate, input power and operating frequency as the code input.

In the right hand side of the momentum and energy equations, the Lorentz force and Joule heating terms are included. The axisymmetric electromagnetic field is assumed as in the flowfeild calculation. Time-averaged values of Lorentz force and Joule heating are calculated by solving Maxwell equations. Technical details are given in Ref. 11. These terms are evaluated at every 1000 times in the CFD calculation by solving the electromagnetic field equations.

Two computational meshes are used to calculate the inductively coupled plasma flowfield: one for the flowfield calculation, and the other for the electromagnetic field. Figure 3 shows the computational grids used in the present study. In the figure, the zone 1 is used for the calculation of the plasma toarch flowfield with 90 x 44 grid points. The farfield boundary for the computational mesh of the electromagnetic field is extended appropriately to impose the boundary condition that electrical and magnetic field is taken to be zero.

B. Boundary Layer Analysis Code

The thermo-chemical nonequilibrium CFD code developed earlier[12] is used for the computation of flowfield over the graphite test piece. The governing equations are the Navier-Stokes equations for axisymmetric flowfield, consisting of species mass, momentum, total energy and vibronic energy conservation equations. The equations are discretized by the cell-centered finite volume scheme utilizing AUSM-DV numerical flux[13] and MUSCL approach for attaining higher order spatial accuracy. Solutions are obtained by integrating the equations in time to steady state using the LU-SGS algorithm.

For high temperature airflow, we employ the following five chemical species, i.e., N, N_2, N^+, N_2^+ and e-. Park's two-temperature model is employed to determine the thermo-chemical nonequilibrium states. The vibronic energy conservation equation accounts for 1) vibrational energy excitation of molecules through collisions between heavy particles, 2) elastic energy transfer between electrons and heavy particles, 3) gains or losses of energy by electron impact ionization, and 4) gains or losses of vibronic energy of heavy particles in chemical reactions.[14] Vibrational relaxation parameters, such as a vibrational relaxation time, are taken from Refs. 15 and 16. The relaxation time is accounted for Park's limiting cross section at high temperature. The values of reaction rate coefficients are taken from Refs. 8 and 15.

A typical example of computational mesh for the flowfield over the test piece is also shown in Fig. 3. The zone 2 with 113 x 69 grid points is used for the calculation. It should be noted that the inlet boundary condition at the entrance of test chamber is given by the solution obtained by the plasma toarch flowfield analysis. As to wall boundary condition at the wall surface of test piece, the constant wall temperature is arbitrary chosen as 500 K. In the present study, the thermo-chemical nonequilibrium CFD code is parallelized with OpenMP directives. All the flowfield calculations are performed using the CFD code on four processors of DELL PRECISION 690. Approximately 100,000 iteration steps are needed to drop the L2-norm of the residual 3 orders of magnitude, requiring about 8 hours of CPU time.

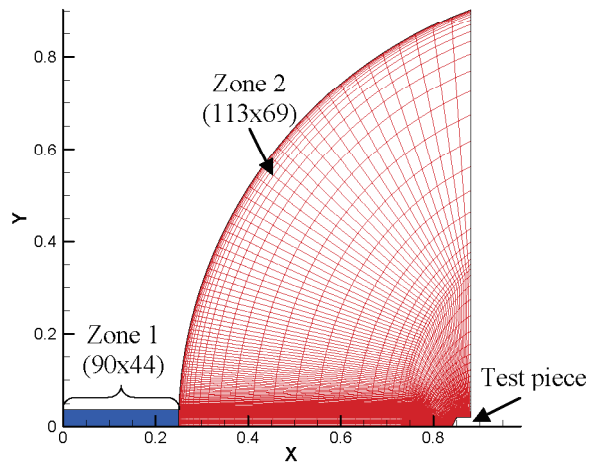

Fig. 3 Computational meshes for 110kW ICP heated wind tunnel facility installed in IAT of JAXA.

IV. Results and Discussions

A. Experimental Results

The heating tests using a graphite test piece are conducted in the 110 kW ICP heated wind tunnel for the wind tunnel test conditions shown in Table 1. Measured surface temperature variations for all test pieces are plotted against time in Fig. 4. As shown in this figure, all temperature variations are within a range between 1700 K and 2000 K, and they are found to be almost constant while heating. The heat up rate is very small, and is approximately 4.8 K/min. Average temperatures are 1953, 1930, 1853 and 1822 K, respectively. For the purpose of simplicity, we hereafter regard the average temperature as temperature of test piece during the heating test.

After the heating tests, graphite test pieces were removed from firebrick attachments, and were weighed to obtain the amount of mass loss of graphite test piece. Obtained weights and mass loss rates of test pieces are summarized in Table 2. A maximum mass loss of about 34% is obtained for the exposure

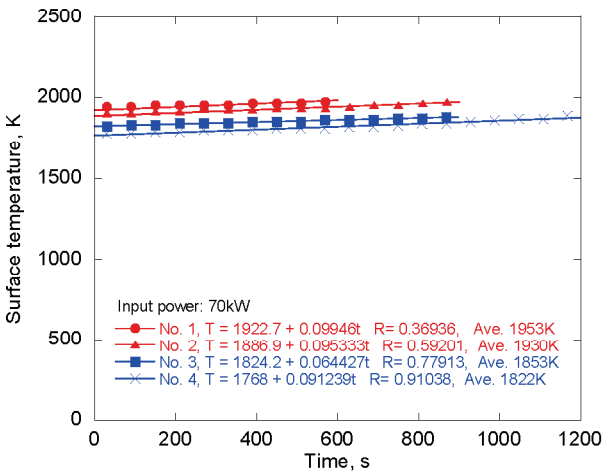

Fig. 4 Time history of surface temperature at the stagnation point.

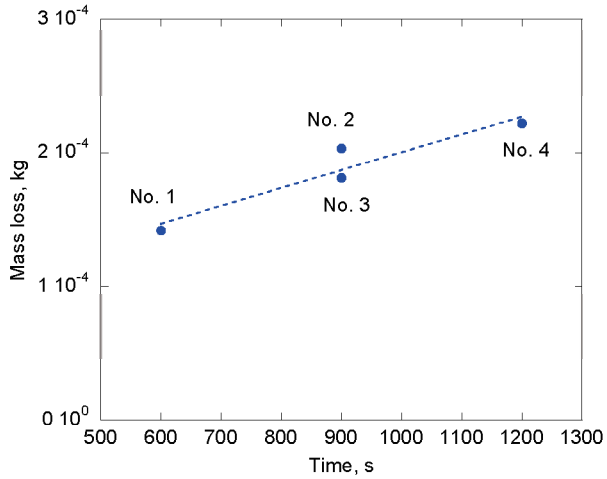

Fig. 5 Comparison of mass loss of graphite test piece.

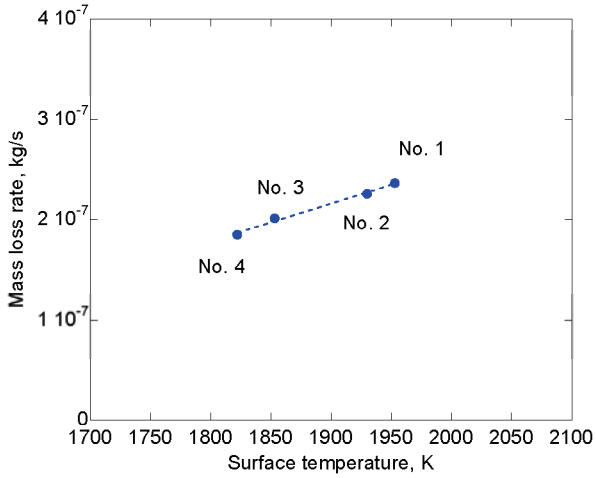

Fig. 6 Mass loss rate plotted against temperature.

Table 2 Mass loss rate of graphite test piecies

Test piece No.	1	2	3	4
Exposure time, [s]	600	900	900	1200
Average temperature, [K]	1953	1930	1853	1822
Mass before heating, [g]	0.6475	0.6478	0.6419	0.6459
Mass after heating, [g]	0.5058	0.4447	0.4609	0.4240
Mass loss [%]	21.88	31.35	28.20	34.36
Mass loss, [kg]	1.417E-4	2.031E-4	1.810E-4	2.219E-4
Mass loss rate, [kg/s]	2.362E-7	2.257E-7	2.011E-7	1.849E-7
Reaction probability	0.00378	0.00363	0.00330	0.00306

time of 1200s. Figure 5 shows the amount of mass loss as a function of exposure time. As shown in Fig. 5, the amount of mass loss of graphite test piece increases with time as expected. Note that the amount of mass loss for the case of test piece No. 2 is larger than that for the case of No. 3 though both of test piecies are heated with same exposure time of 900 s. This difference is due to the fact that the surface temperature for the case of No. 2 is higher than that for the case of No. 3, as shown in Fig. 4. As a result, the mass loss rate for the case of No. 2 becomes larger than that for the case of No. 3. The mass loss rate of graphite test piece obtained in this study are plotted against surface temperature in Fig. 6. From the figure, one can see that mass loss rate of graphite increases as temperature increases.

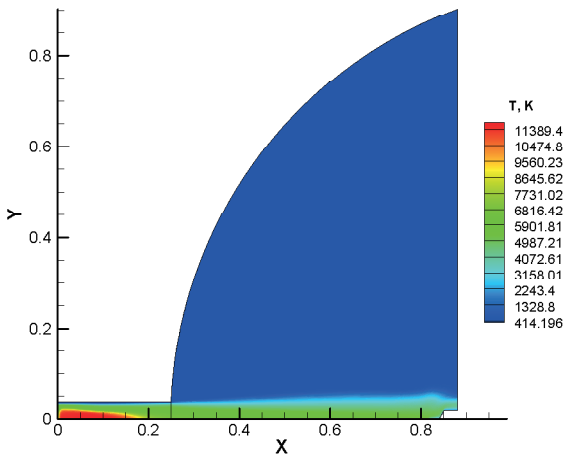

Fig. 7 Computational meshes for 110kW ICP heated wind tunnel facility installed in IAT of JAXA.

B. Numerical Results

In order to evaluate atomic nitrogen density in the test section, numerical analysis around the test piece is made under the ICP wind tunnel test condition. Inlet boundary condition at the entrance of the test chamber is given by the solution obtained by the plasma toarch flowfield analysis. Figure 7 shows typical example of temperature contours for the converged solution. Because of significant heating in the plasma toarch, the temperature becomes larger than 10,000 K, and then gradually decreases toward the test piece.

Calculated temperature, density and species concentrations along the stagnation line in the test chamber are shown in Figs. 8(a)-8(c), respectively. For the purpose of comparison, measured values using radiation spectroscopy by Fujita et al.[10] are given in the same figures. In the work by Fujita et al., radiation spectroccopy of flows in the ICP heated wind tunnel is conducted to evaluate the flow properties in the test section. The measurements are made at 372mm from the coil center (at 364mm from the test piece). By comparing the measured spectrum with that calculated by using the computer code named SPRADIAN2, molecular temperature and species concentrations are determined for nitrogen test flow at the wind tunnel test condition of 90 kW. Although the measured values were obtained for different input power condition from the present study, it is found from Figs. 8(a)-8(c) that the agreement between the calculation and the measurement is fairly good.

As shown in Fig. 8(a), a maximum temperature value of about 6800 K is obtained at the entrance of test chamber, and then gradually decreases toward the test piece. One can also see from Fig. 8(a) that thermal equilibrium is

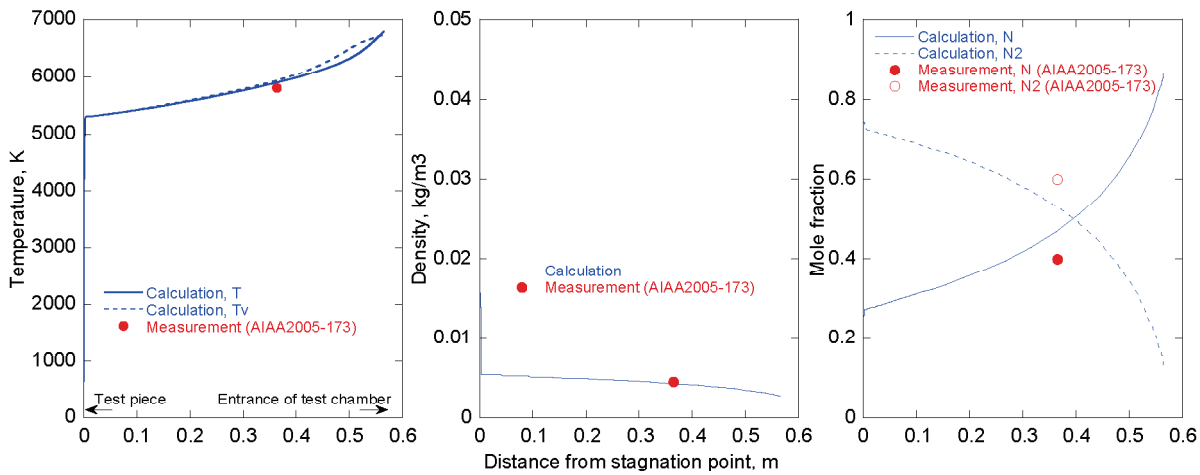

(a) Temperature **(b) Density** **(c) Mass concentration**

Fig. 8 Flow properties along stagnation line.

reached in the entire region. Figure 8(c) represents the mole fraction of atomic and molecular nitrogen. From this figure, one can see that recombination of atomic nitrogen occurs along the stagnation line. The mole fraction of atomic nitrogen at the test piece surface is about 0.25. From Figs. 8(b) and 8(c), atomic nitrogen density at the test piece surface for the present heating condition is estimated, and is found to be 7.0×10^{-4} kg/m^3.

C. Probability of Nitridation Reaction

We first consider the reaction probabirity of nitridation reaction for the case of test piece No. 1. In Fig. 9, Eq. (5) is plotted as a function of reaction probability with the surface temperature of 1953 K and the atomic nitrogen density of 7.0×10^{-4} kg/m^3. For the purpose of comparison, Eq. (5) with the atomic nitrogen densities of 7.0×10^{-3} and 7.0×10^{-5} kg/m^3 is also shown in the same figure. As shown in this figure, the smaller density we assume, the larger reaction probability becomes. The reaction probability is then found to be 0.00378 with the density value calculated in this study.

The reaction probability values for all test piecies are plotted against reciprocal temperature in Fig. 10. The results obtained by Park and Bogdanoff[6] and the reaction probability for the oxidation reaction in Eq. (1), taken from Ref. 7, are also shown for comparison. The reaction probability values obtained in this study are 0.00378, 0.00363, 0.00330 and 0.00306, respectively. Those values are also shown in Table 2. From the figure, one can see that the probability values of nitridation reaction are smaller that those of oxidation reaction.

As Fig. 10 shows, the reaction probability obtained in this study is substantially smaller than that obtained by Park and Bogdanoff. The exact reason for this distinction remains uncertain. However, in order to examine the reaction probability in the course of the present study, more work will be needed. Because the thermochemical state in the boundary layer is affected by the surface reaction product, CN, the amount of atomic nitrogen around the test piece will be changed. This modification in turn affects the amount of mass loss of test piece. Such effects are not included in the calculation made in this study. In addition, because surface shape of test piecies changes due to the nitridation reaction during the heating tests, constant surface area assumption made in this study will be no more reasonable. In order to examine these effects, and to estimate the flow density more accurately, the flowfield around the test piece need to be calculated by coupling with the thermal response calculation of the test piece. Such coupled calculation will be made in the future.

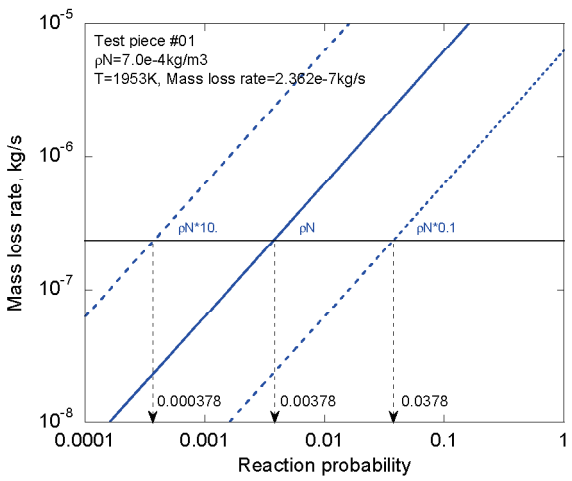

Fig. 9 Mass loss rate obtained in this study for the case of test piece No. 1.

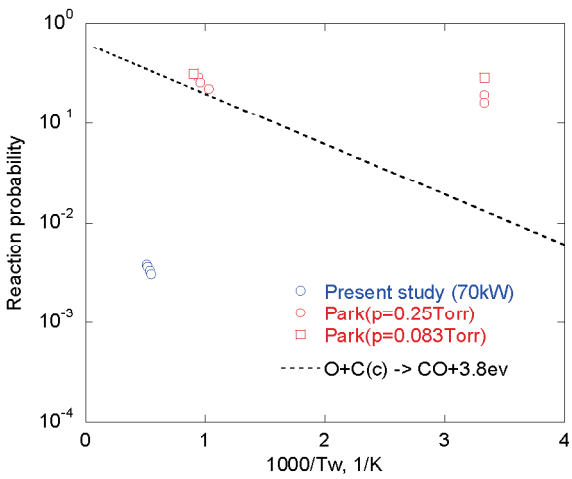

Fig. 10 Nitridation reaction probability values plotted against reciprocal temperature.

V. Conclusions

Heating tests are conducted in the 110kW ICP heated wind tunnel in IAT of JAXA. In the tests, graphite test piecies are exposed to nitrogen test flow. Mass loss of test piecies due to nitridation reaction are measured after the heating tests. A maximum mass loss of about 34% is obtained for the exposure time of 1200s. In order to evaluate the flow properties in the test section, the flowfield around the test piece is calculated under wind tunnel freestream condition. The freestream condition is evaluated by calculating the flows in the ICP heater fully theoretically. From

the study, the atomic nitrogen density at the stagnation point is found to be 7.0×10^{-4} kg/m^3. Using the amount of mass loss of test piece and atomic nitrogen density so evaluated, the reaction probability of nitridation is determined. The obtained probability value is about 0.003 for the temperature of about 1900K. It is found out that probability obtained in this study is about 1/100 smaller than that obtained by Park and Bogdanoff.

The present work relies partly on the accuracy of estimated flow density. More work will be needed to evaluate the amount of the atomic nitrogen around the test piece. It is desiable that the flowfield in the test section is calculated by accounting for the surface reaction product and shape change of test piece during the heating tests.

Acknowledgments

The first author appreciates various technical suggestions for the experiment given by Messrs. Kiyomichi Ishida, Junsei Nagai and Masashi Taniguchi of the Wind Tunnel Technology Center of JAXA. This work was partly supported by the Grant-in-Aid for Young Scientists (B) (No. 18760613) from the Ministry of Education, Culture, Sports, Science and Technology in Japan.

References

[1]Working Group of Asteroid Sample Return Mission, "A Program of Exploring an Asteroid (MUSES-C), The Proposal," Institute of Space and Astronautical Science, Kanagawa, Japan, March 1995.

[2]Institute for Unmanned Space Experiment Free Flyer, "Unmanned Space Experiment Recovery System," URL: http://www.usef.or.jp/English/f3_project/users/f3_users.html [cited 12 March 2006].

[3]Rosner, D. G., and Allendorf, H. D., "Comparative Studies of the Attack of Pyrolytic and Isotropic Graphite by Atomic and Molecular Oxygen at High Temperatures," *AIAA Journal*, Vol. 6, April 1965, pp. 650-654.

[4]Marsh, H., O'Hair, T. E., and Wynnes-Jones, L., "The Carbon-Atomic Oxygen Reaction Surface-Oxide Formation on Paracrystalline Carbon and Graphite," *Carbon*, Vol. 7, May 1969, pp. 555-566.

[5]Lundell, J. H., and Dickey, R. R., "Ablation of ATJ Graphite at High Temperatures," *AIAA Journal*, Vol. 11, Feb. 1973, pp. 216-222.

[6]Park, C., and Bogdanoff, D. W., "Shock-Tube Measurement of Nitridation Coefficient of Solid Carbon," *Journal of Thermophysics and Heat Transfer*, Vol. 20, No. 3, 2006, pp. 487-492.

[7]Park, C., "Effect of Atomic Oxygen in Graphite Ablation," *AIAA Journal*, Vol. 14, No. 11, 1976, pp. 1640-1642.

[8]Park, C., Jaffe, R. L., and Partridge, H., "Chemical-Kinetic Parameters of Hyperbolic Earth Entry," *Journal of Thermophysics and Heat Transfer*, Vol. 15, No. 1, 2001, pp. 76-90.

[9]Suzuki, T., Sakai, T., and Yamada, T., "Calculation of Thermal Response of Ablator Under Arc-Jet Flow Condition," *Journal of Thermophysics and Heat Transfer*, Vol. 21, No. 2, 2007, pp. 257-266.

[10]Fujita, K., Mizuno, M., Ishida, K., Ito, T., Sumi, T., and Kurotaki, T., "Spectroscopic Diagnostics of Electrically Heated High Enthalpy Wind Tunnels," AIAA Paper 2005-173, 43rd AIAA Aerospace Sciences Meeting and Exhibit, Reno, NV, Jan. 10-13, 2005.

[11]Ando,K., Sakai, T., and Yamada, T., "Calculation of Flows in an Inductively Coupled CO_2 Plasma Wind Tunnel," Symposium on Flight Mechanics and Astrodynamics, 2006, in Japanese

[12]Suzuki, T., Furudate, M., and Sawada, K., "Unified Calculation of Hypersonic Flowfield for a Reentry Vehicle," *Journal of Thermophysics and Heat Transfer*, Vol. 16, No. 1, 2002, pp. 94-100.

[13]Wada, Y., and Liu, M. S., "A Flux Splitting Scheme with High Resolution and Robustness for Discontinuities," AIAA Paper 94-0083, Jan. 1994.

[14]Park, C., *Nonequilibrium Hypersonic Aerothermodynamics*, John Wiley and Sons Inc., New York, 1989

[15]Park, C., "Review of Chemical-Kinetic Problems of Future NASA Missions. I: Earth Entries," *Journal of Thermophysics and Heat Transfer*, Vol. 7, No. 3, 1993, pp. 385-398.

[16]Park, C., Howe, J. T., Jaffe, R. L., and Candler, G. V., "Chemical-Kinetic Problems of Future NASA Missions. II. Mars Entries: A Review," *Journal of Thermophysics and Heat Transfer*, Vol. 8, No. 1, 1994, pp. 9-23.